

Succinct Papers

Shaped-Conical Radiation Pattern Performance of the Backfire Quadrifilar Helix

CHARLES C. KILGUS

Abstract—It is shown that shaped-conical radiation patterns can be realized by extending the resonant fractional-turn quadrifilar helix to an integral number of turns, i.e., the radiated energy can be concentrated into a cone with the gain decreasing from a maximum at the edge of the cone to a local minimum at the center. This pattern shape is near optimum for many spacecraft communications and navigation applications, providing approximately 3 dB improvement over cardioid shaped patterns.

INTRODUCTION

The fractional-turn resonant quadrifilar helix produces a cardioid shaped radiation pattern with excellent circular polarization over a wide angle. This antenna has found application in a number of spacecraft programs because of its small size, lack of a ground plane, and insensitivity to nearby metal structure [1]–[3].

It is desirable in many satellite and ground station applications to concentrate the radiated energy into a cone with 120° to 180° total cone angle. The optimum is a “shaped-conical” radiation pattern with a maximum gain at the rim of the cone and gain decreasing to a minimum of approximately 10 dB less at the center of the cone (this produces uniform signal strength at the receiver throughout the satellite pass).

This paper describes the shaped-conical beams that can be realized by extending the fractional-turn quadrifilar helix to an integral number of turns. The radiation is backfire, i.e., toward the feed point. Shaped-conical radiation patterns with full-cone angles from 100° to 180° and center minimums down 3 dB to 20 dB can be realized by the proper choice of helical parameters. Measured radiation pattern data is presented for helices with one to five turns.

Many investigators have studied various forms of the helix antenna but the backfire helix has received relatively little attention (probably because it provides highly directive beams only over a narrow bandwidth). Patton demonstrated that the long backfire bifilar helix produces shaped conical beams; that the beam scans from backfire to broadside as the size of the antenna in wavelengths increases; and that the front-to-back ratio degrades to unity as the number of turns decreases to one [4]. The backfire quadrifilar helix described in this paper maintains its electrical performance and in particular maintains an excellent front-to-back ratio even for a fractional number of turns. Adams *et al.*, describe work done on the essentially different high gain forward fire quadrifilar helix fed against a ground plane and provide a bibliography of helix research [5].

HELIX DESCRIPTION

Each of the four elements of the quadrifilar helix consists of a helical portion and two radial portions (Fig. 1). The four top radials connect the helical portions to the feed region, the

bottom radials are carried to the center and shorted together.

At the feed region opposite elements are fed in antiphase to produce two independent bifilar helices. The bifilar helices are fed in phase quadrature to produce the quadrifilar helix.

The helix can be described by the parameters:

r_0 radius in wavelengths,

p pitch distance for one element measured along the axis of the helix,

N number of turns for one element.

The parameter k is then the ratio

$$k = \frac{r_0}{p}$$

and the axial length of the helix is

$$L_{ax} = pN.$$

The length along one element L_{ele} is related to the other parameters by

$$p = \sqrt{\frac{1}{N^2} (L_{ele} - 2r_0)^2 - 4\pi^2 r_0^2}.$$

TYPICAL RADIATION PATTERNS

A typical shaped-conical radiation pattern can be described by the following three parameters (Fig. 2).

θ_{BW} beamwidth from the center of the cone to the 3 db point outside the pattern maximum. Note that this is the ordinary 3-dB beamwidth if the pattern maximum is along the cone axis.

θ_p angle between the cone axis and the peak of the radiation pattern.

α_{db} depth of the pattern minimum at $\theta = 0^\circ$ relative to the pattern maximum. Patterns with a secondary minimum significantly below the level at $\theta = 0^\circ$ are noted.

MEASURED DATA

Region of Shaped Conical Beams: The measured data indicated that the parameter range for shaped-conical beams is bounded by regions of unsatisfactory performance (Fig. 3). Helices with too small pitch and diameter fall in a region of narrow beams with no center minimum. When only the diameter is too small, shaped-conical beams result for moderate pitch spacings but multiple lobes appear for large pitch spacings. Too large diameters produce conical beams with no center minimum and a tendency to have ripples and other distortion. Finally, a too large pitch spacing produces beamwidths greater than 180°.

The Data Set: Pattern data was measured over the region of shaped-conical beams for helices with $k = 0.038, 0.083$, and 0.164 , for $N = 1, 2, 3$, and 5 turns. The angle to the peak, beamwidth, and depth of the center minimum are presented in Fig. 4–7; some typical radiation patterns are included as Fig. 8. Data was also taken on a helix with $k = 0.3$, but no beam shaping was evident and it is not presented here. Data was taken on the helix with $k = 0.164$ and $N = 7$ turns but it was similar to the data for $N = 5$ turns and is not presented.

Manuscript received September 16, 1974; revised December 13, 1974.

The author is with the Applied Physics Laboratory, Johns Hopkins University, Silver Spring, Md. 20910.

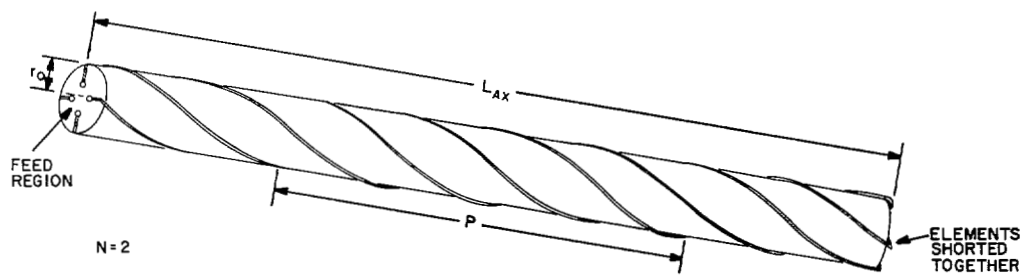


Fig. 1. Helical parameters.

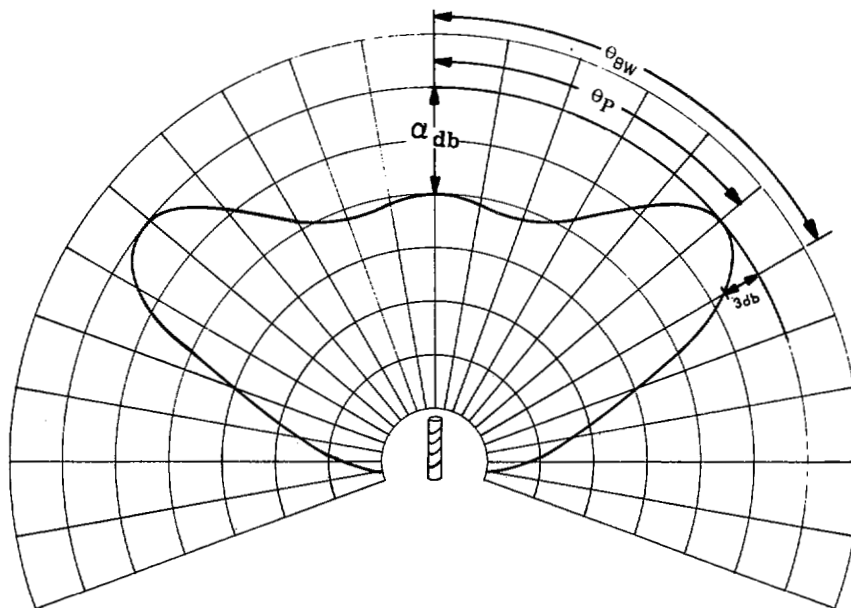


Fig. 2. Typical radiation pattern shaped-conical beam quadrifilar helix.

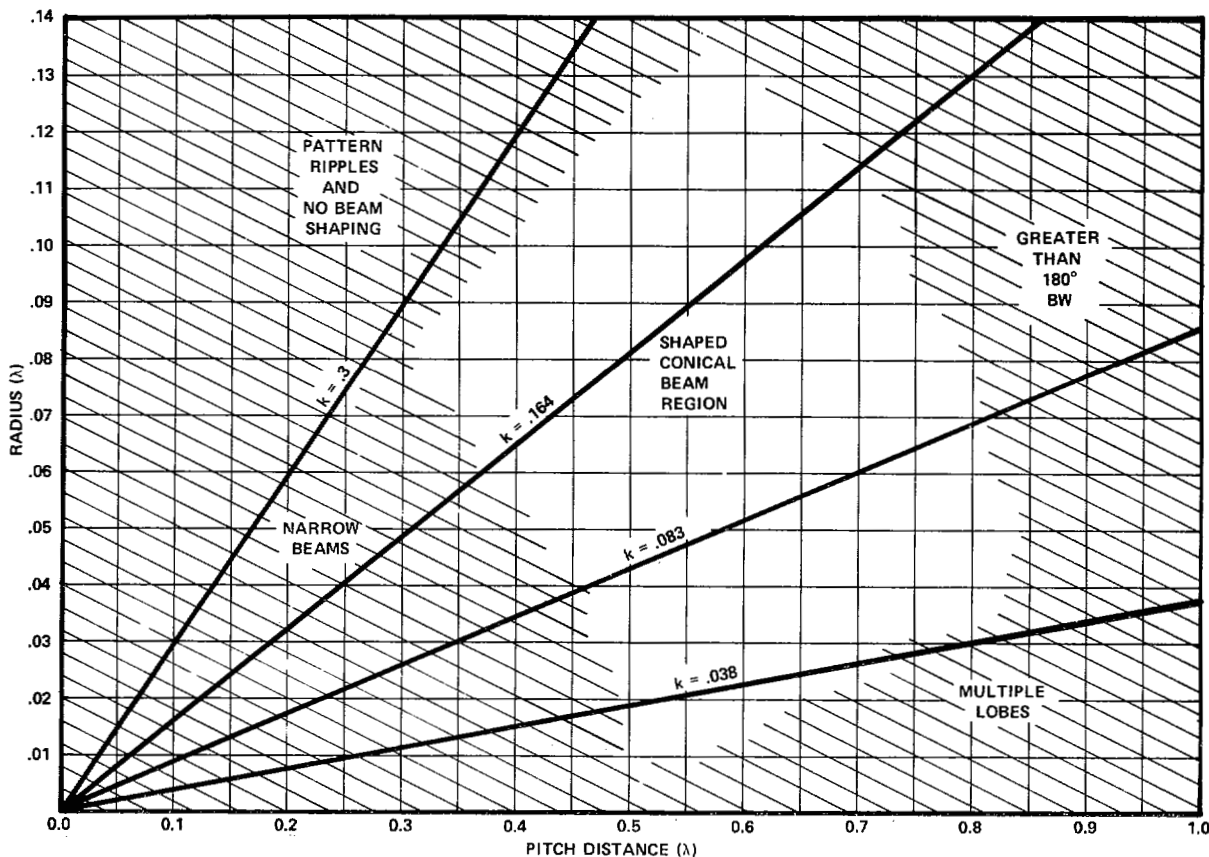
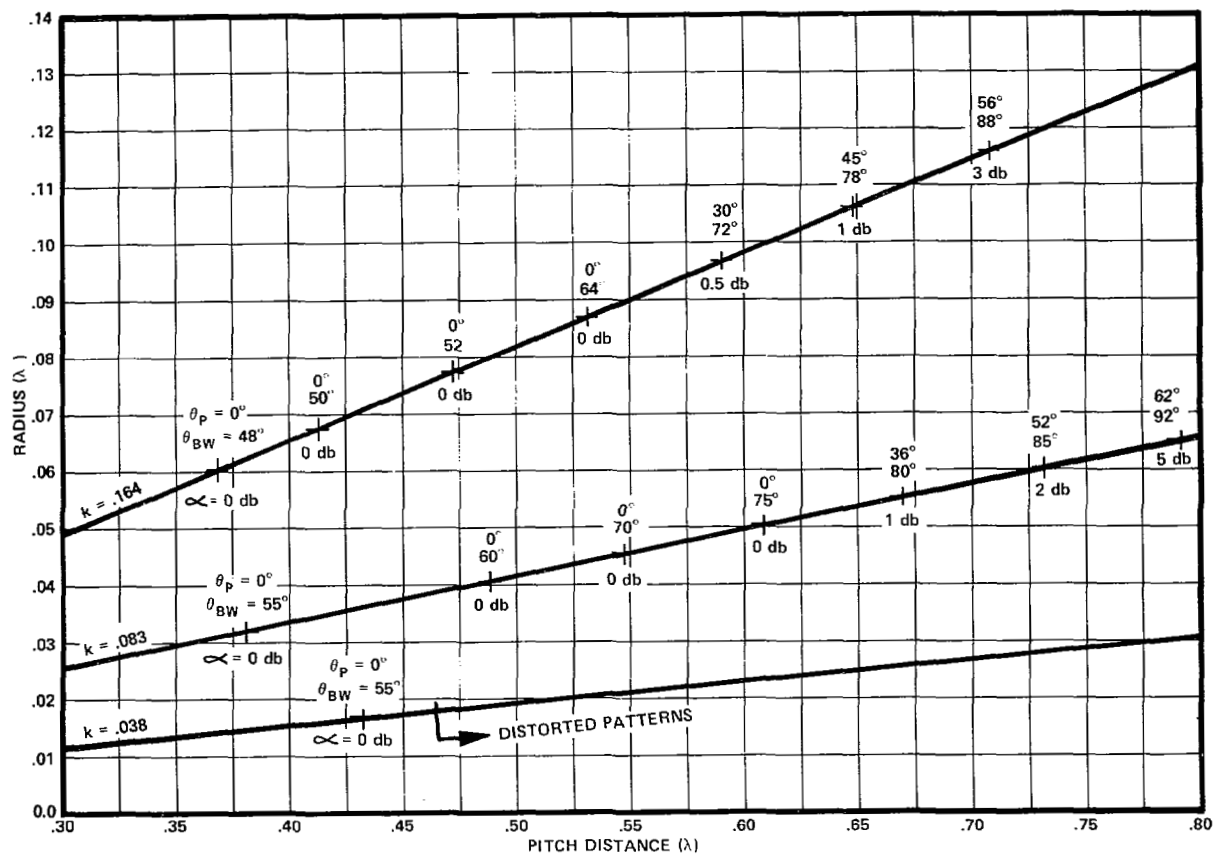
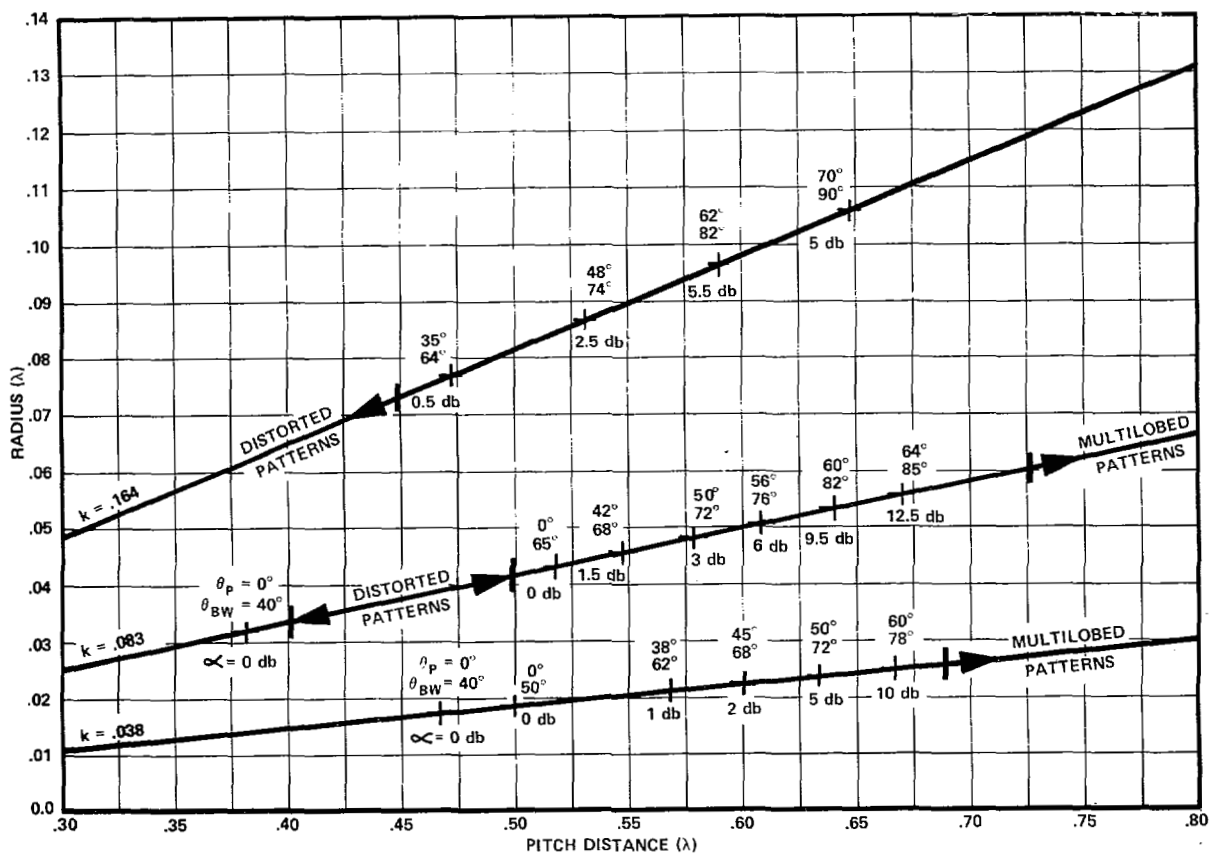
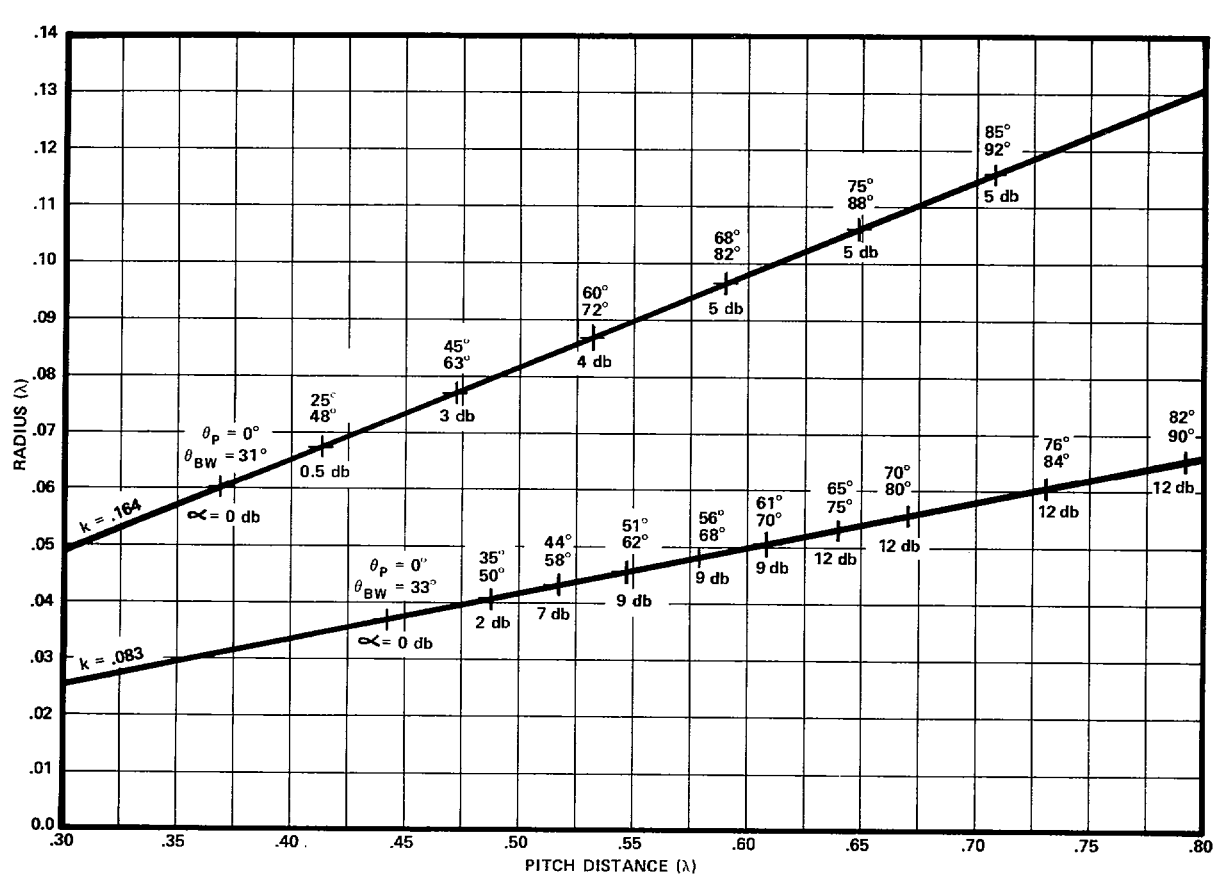
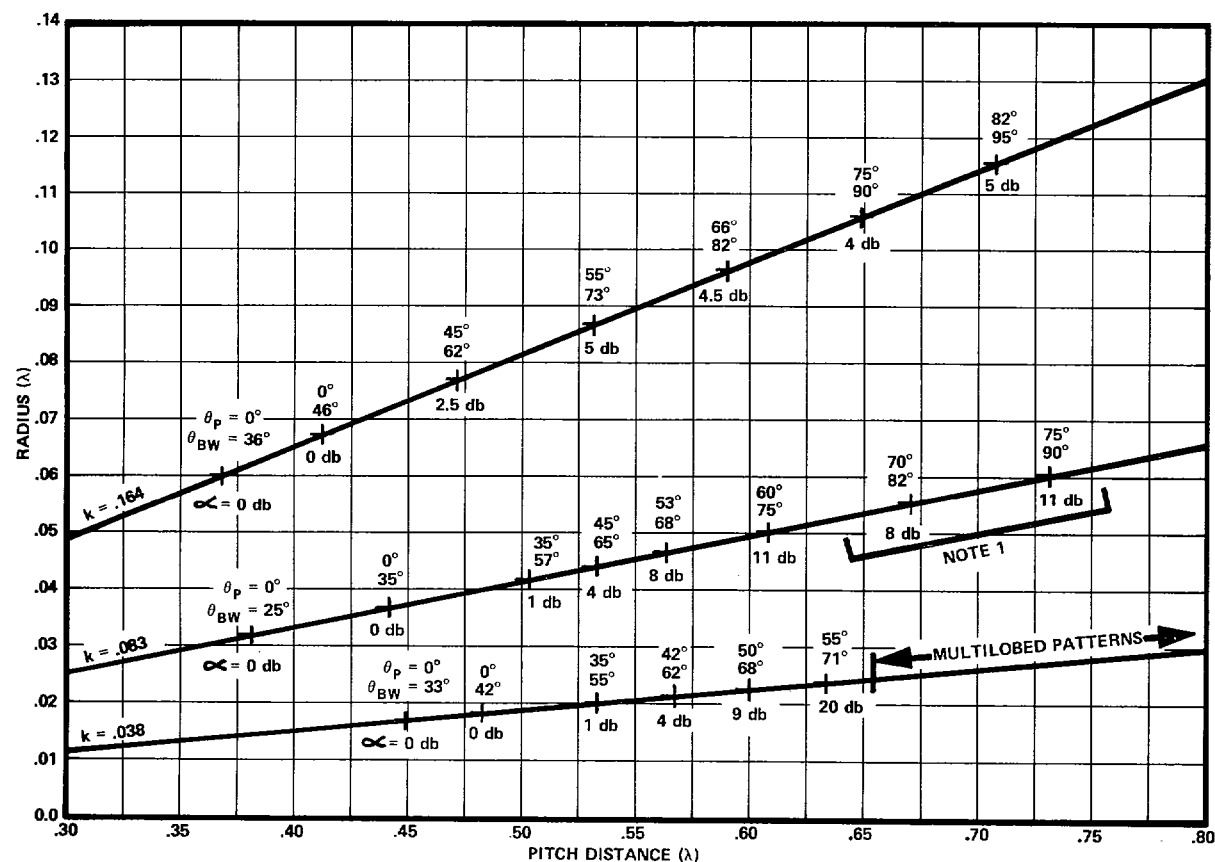
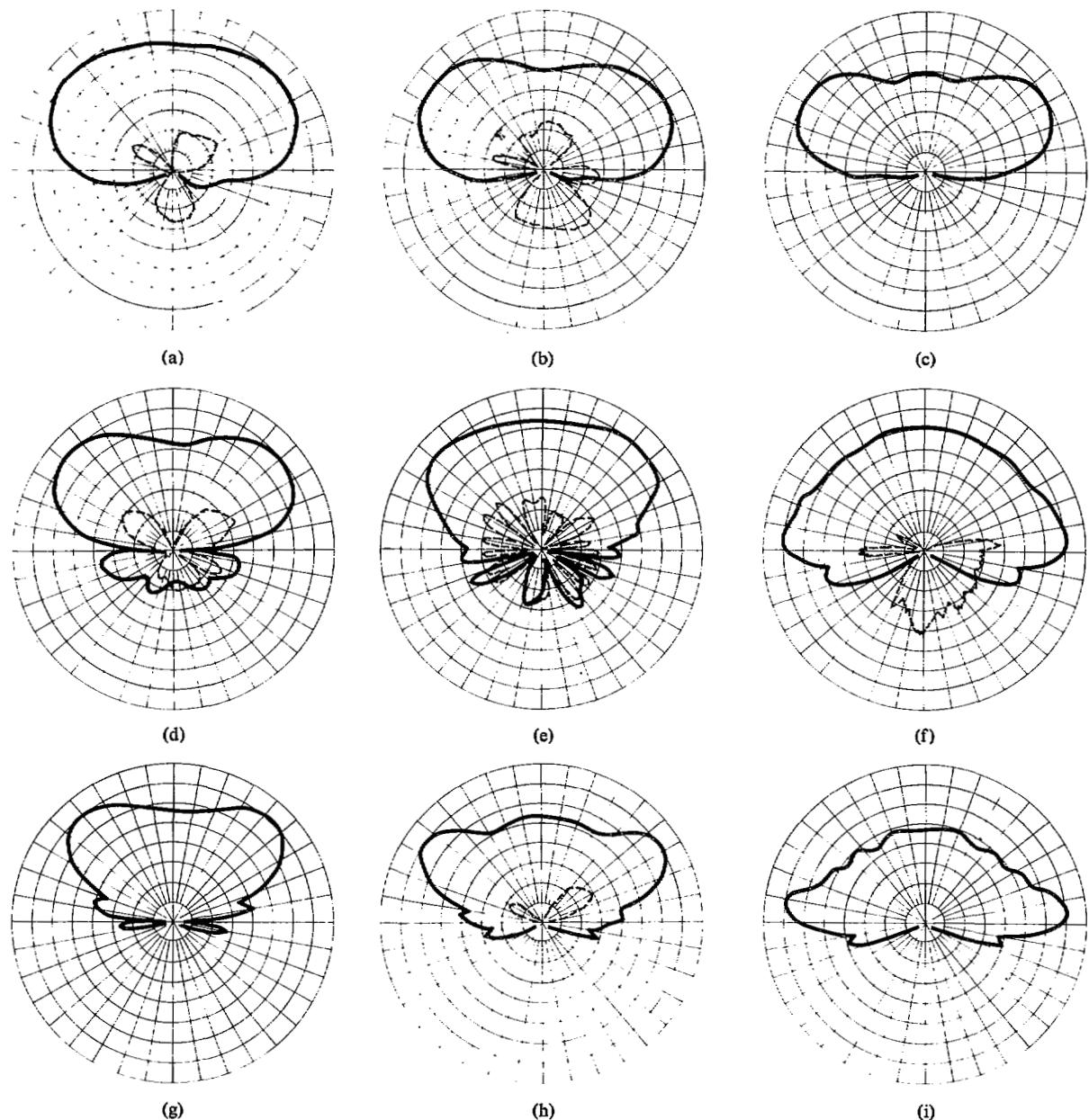


Fig. 3. Region of shaped conical beam performance.

Fig. 4. Radiation pattern characteristics for $N = 1$ turn.Fig. 5. Radiation pattern characteristics for $N = 2$ turns.

Fig. 7. Radiation pattern characteristics for $N = 5$ turns.



Circular polarization, 5 dB/division, measured radiation patterns (— left-hand circular, - - - right-hand circular).
 (a) 2 turns, $k = 0.083$, $p = 0.59$. (b) 2 turns, $k = 0.038$, $p = 0.667$. (c) 3 turns, $k = 0.083$, $p = 0.609$. (d) 3 turns, $k = 0.083$, $p = 0.600$. (e) 5 turns, $k = 0.164$, $p = 0.472$. (f) 5 turns, $k = 0.164$, $p = 0.707$. (g) 5 turns, $k = 0.083$, $p = 0.518$. (h) 5 turns, $k = 0.083$, $p = 0.579$. (i) 5 turns, $k = 0.083$, $p = 0.792$.

Fig. 8. Measured radiation pattern.

Description of the Data: Both the front-to-back ratios and axial ratios of the circular polarization were generally excellent over the entire data set; measuring usually 10 to 15 dB and 3 to 6 dB, respectively.

No systematic impedance data was measured but the radiation pattern levels indicated that the helices with element lengths shorter than 1 wavelength were sharply resonant. Helices with element lengths of several wavelengths gave no indication of resonant characteristics; limited data indicates an input impedance from 100 to 300 Ω .

As the data indicates, little beam shaping occurred for any choice of parameters when $N = 1$ turn. When $N = 3$ turns or 5 turns (helices with axial lengths of 1.5 to 2 wavelength or 2 to 3 wavelengths, respectively) well formed shaped-conical beams

are produced. In particular the helix with $N = 5$, $k = 0.083$, $p = 0.579$ produces a pattern that is nearly optimum for a satellite in a 600-nmi orbit (Fig. 8(h)); the helix with $N = 5$, $k = 0.164$, $p = 0.708$ produces a nearly hemispherical pattern (Fig. 8(f)) as required for a nonpointed ground station antenna. The pattern of Fig. 8(h) has a directivity of 7 dB, providing a gain of 3 dB (at the edge of the visible earth) over a cardioid pattern covering the same angle.

Description of the Test Antennas: The test antennas were constructed by winding four equal length RG142 coaxial cables on light wooden frames. The bifilar helices were realized by utilizing two adjacent coaxial lines as feed cables and connecting their center conductors to the shield of the opposite cable at the

feed point at the top of the helix; producing two frequency independent "infinite baluns."

Only the shields of the opposite cables are used to complete the bifilar helices, the center conductors are not connected at either end. The four shields are shorted together at the bottom of the helix. The feed cables continue and are connected to wide band 3-dB directional couplers to produce the desired phase quadrature between bifilar helices. Each antenna was tested over a 2.5:1 frequency band in the VHF-UHF region to produce data along a constant k line on the r_0, p diagram.

ACKNOWLEDGMENT

The author acknowledges the diligence and insight of C. Webster and W. Potter in constructing the test antennas and in organizing and conducting the test program.

REFERENCES

- [1] C. C. Kilgus, "Spacecraft and ground station applications of the resonant quadrifilar helix," *Digest of the 1974 Int. IEEE/AP-S Symp.*, June 1974, pp. 75-77.
- [2] —, "Resonant quadrifilar helix design," *Microwave J.*, vol. 13-12, pp. 49-54, Dec. 1970.
- [3] —, "Resonant quadrifilar helix," *IEEE Trans. Antennas Propagat. (Commun.)*, vol. AP-17, pp. 349-351, May 1969.
- [4] W. T. Patton, "The backfire bifilar helical antenna," Univ. of Illinois Antenna Lab Rep. 61, Sept. 1962 (AD 289084).
- [5] A. T. Adams, R. K. Greenough, R. F. Wallenberg, A. Mendelovitz, and C. Lumjiak, "The quadrifilar helix antenna," *IEEE Trans. Antennas Propagat.*, vol. AP-22, pp. 173-178, Mar. 1974.

Analysis of the Log-Periodic V-Dipole Antenna

K. K. CHAN AND P. SILVESTER

Abstract—The log-periodic V-dipole antenna (LPVA) operating in the $3\lambda/2$ mode is analyzed numerically using the projective technique. The antenna is treated as a parallel connection of an array of V-dipoles and a feeder transmission line. This decoupling of the circuits enables one to obtain the dipole currents simply by considering the array of V-dipoles as a boundary value problem and solving the necessary integral equations. The currents can then be used to give the various properties of the antenna. Effects on the antenna behavior obtained by changing its parameters are illustrated, and general characteristic curves presented.

I. INTRODUCTION

From a survey of the literature, very few detailed studies of the log-periodic V-dipole antenna (LPVA) were found to exist, most studies being based on the log-periodic dipole antenna (LPDA). Mayes' and Carrel's treatment [1] of the LPVA is mainly experimental. From their studies, certain general requirements could be deduced for the successful operation of the LPVA's. It is the purpose of this paper to provide more complete information so that one may predict more accurately the behavior of the antenna once its parameters are specified.

Only the single $3\lambda/2$ mode operation of the LPVA is investigated here. Its operation is similar to that of the LPDA [2] except that the active region is now centered among dipoles $3\lambda/2$ long and the arms of the dipoles are bent forward to increase the antenna directivity.

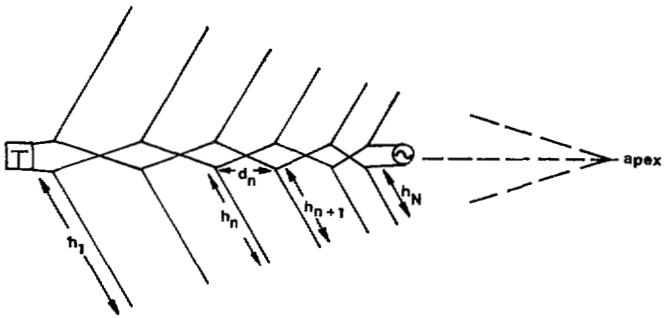


Fig. 1. Log-periodic V-dipole antenna.

The current distributions on the dipole elements are obtained by the projective method, which has been used successfully for the solution of the LPDA [3]. The effectiveness of the projective method, as compared to methods available, is in part due to the use of relatively long wire elements with the appropriate current approximating polynomials to model antenna structures. This is particularly true in the case of the LPVA, which, depending upon its mode of operation and structural bandwidth, may contain dipole elements many wavelengths long. Fewer wire elements are thus needed to model it, resulting in smaller matrix equations for solution.

II. MATRIX SOLUTION OF LPVA

The geometry of the LPVA is shown in Fig. 1. The parameters that describe the LPVA are scaling factor τ , spacing factor σ , length to diameter ratio h/a , feeder line impedance Z_f , feeder terminating impedance Z_t , and ψ , the angle between the arms. For a tractable formulation of the problem, the LPVA is considered as a parallel connection of two electrically decoupled circuits, the antenna element circuit and the feeder circuit.

Let Z_a and Y_f be the impedance matrix of the antenna circuit and admittance matrix of the feeder circuit, respectively. It can be shown that the input driving current, set equal to 1 A here, is related to the base currents of the dipole elements by the following

$$I = [U + Y_f Z_a] I_a \quad (1)$$

where $I = [0 \ 0 \ \dots \ 1]^T$. Arrays I and I_a have dimensions $N \times 1$ while those of Y_f and Z_a are $N \times N$, where N is the number of dipole elements.

The calculation of the admittance matrix for the feeder circuit is straightforward. Its expression is given in [4] and will not be repeated here. On the other hand, calculation of the port impedance matrix Z_a is slightly more involved. It is derived from the generalized impedance matrix whose formulation is based on the projective solution of the current integral equations. The steps required for the projective solution are clearly delineated in [5].

Let GZ represent the generalized impedance matrix of the antenna elements. Its rows and columns, which correspond to the feed points of the dipole elements, may be rearranged and partitioned so that the general matrix equation is transformed into the following:

$$\begin{bmatrix} GZ_{11} & | & GZ_{12} \\ \hline GZ_{21} & | & GZ_{22} \end{bmatrix} \begin{bmatrix} I_1 \\ I_a \end{bmatrix} = \begin{bmatrix} V_1 \\ V_a \end{bmatrix} \quad (2)$$

where I_a and V_a are the currents and voltages at the feed points, i.e., at the bases of the dipole elements. Since V_1 are the impressed voltages on the rest of the dipole elements, they are all equal to zero. Manipulation of the partitioned matrices results in the